MAD2 haplo-insufficiency causes premature anaphase and chromosome instability in mammalian cells

Loren S. Michel*†‡, Vasco Liberal†‡, Anupam Chatterjee§, Regina Kirchwegger‡, Boris Pasche‖, William Gerald¶, Max Dobles#, Peter K. Sorger#, V. V. V. S. Murty§ & Robert Benezra‡

** Department of Medicine, and ¶ Department of Pathology, Memorial Sloan-Kettering Cancer Center, New York, New York 10021, USA*
‡ Cell Biology and Genetics Program, Memorial Sloan-Kettering Cancer Center and the Sloan-Kettering Division, Graduate School of Medical Sciences, Cornell University, New York, New York 10021, USA
§ Department of Pathology, College of Physicians and Surgeons of Columbia University, New York, New York 10032, USA
‖ Division of Hematology/Oncology and Robert H. Lurie Comprehensive Cancer Center, Northwestern University Medical School, Chicago, Illinois 60611, USA
 # Biology Department, Massachusetts Institute of Technology, Cambridge, Massachusetts 02139, USA
† These authors contributed equally to this work

The mitotic checkpoint protein hsMad2 is required to arrest cells in mitosis when chromosomes are unattached to the mitotic spindle[1]. The presence of a single, lagging chromosome is sufficient to activate the checkpoint, producing a delay at the metaphase–anaphase transition until the last spindle attachment is made[2]. Complete loss of the mitotic checkpoint results in embryonic lethality owing to chromosome mis-segregation in various organisms[3–6]. Whether partial loss of checkpoint control leads to more subtle rates of chromosome instability compatible with cell viability remains unknown. Here we report that deletion of one *MAD2* allele results in a defective mitotic checkpoint in both human cancer cells and murine primary embryonic fibroblasts. Checkpoint-defective cells show premature sister-chromatid separation in the presence of spindle inhibitors and an elevated rate of chromosome mis-segregation events in the absence of these agents. Furthermore, *Mad2*$^{+/-}$ mice develop lung tumours at high rates after long latencies, implicating defects in the mitotic checkpoint in tumorigenesis.

Genetic instability in cancers occurs frequently with whole chromosomes, referred to as chromosome instability (CIN)[7]. CIN cells become aneuploid (that is, they acquire abnormal chromosome numbers), a hallmark of cancer that is associated with aggressive tumour behaviour and a poor prognosis[8]. Aneuploidy may facilitate tumorigenesis or tumour progression through the loss of tumour-suppressor gene function. The mechanisms responsible for the development of aneuploidy in cancers remain unclear. Defects in the mitotic checkpoint have been correlated with CIN in human cancer cells but have not yet been shown to be a direct cause of the CIN phenotype[9]. We therefore investigated whether the loss of *MAD2* through targeted deletion in a cancer cell line that is chromosomally stable would result in its transformation into a CIN line. We chose the Hct-116 human colon carcinoma cell line because it has a normal mitotic checkpoint and is amenable to gene targeting[9–11].

We generated two independent Hct-*MAD2*$^{+/-}$ clones for analysis (For details of the vector design and genomic analysis, see Supplementary Information). We exposed asynchronous Hct-*MAD2*$^{+/-}$ cells to nocodazole and then measured the mitotic index by staining them with MPM-2, a mitosis-specific antigen. Sixty per cent of wild-type cells arrest by 18 h, whereas only 10% of mutant cells do so (Fig. 1a). Consistent with the loss of the mitotic checkpoint, 77% of mutant cells proceed into a subsequent S phase, as assayed by DNA content, compared with 36% of wild-type cells (Fig. 1b). The checkpoint defect of *MAD2*$^{+/-}$ cells was confirmed by assaying cyclin-B-associated Cdc2 kinase activity of G1/S synchronized cell populations that had been released into nocodazole. Wild-type cells show high levels of Cdc2 kinase activity for 24 h, whereas the kinase activity of mutant cells falls rapidly after 12 h in nocodazole (Fig. 1c, d). This fall in kinase activity is accompanied by the acquisition of 8*N* DNA content (where *N* is the amount of DNA in a haploid cell), as mutant cells proceed through the next cell cycle (Fig. 1e). After 24 h, most of the wild-type cells have rounded up and detached from the culture dish, whereas mutant cells remain adherent as they continue to cycle (Fig. 1f, g). On prolonged exposure to nocodazole (over 48 h), mutant cells become multinucleated with a polyploid DNA content (Fig. 1h).

To ensure that the phenotype observed in Hct-*MAD2*$^{+/-}$ cells was not the result of the transfection or selection process, two selected clones that had not recombined homologously were challenged with nocodazole and found by MPM-2 staining to arrest in mitosis identically to Hct-116 non-transfected controls (data not shown). Immunoblots against MAD2 with polyclonal anti-sera show one species with a relative molecular mass of 27,000 (M_r 27K) in both Hct-*MAD2*$^{+/-}$ clones, indicating that there is not a dominant-negative effect of a partial protein product. Quantitative iodinated immunoblots normalized to Cdk2 show that Hct-*MAD2*$^{+/-}$ cells express 70% of the amount of MAD2 protein expressed in wild-type cells, suggesting partial compensation of protein levels in the absence of one allele (see Fig. 2, Supplementary Information,). We found that the expressed allele is wild type by polymerase chain reaction with reverse transcription of RNA and subsequent sequence analysis. Finally, the checkpoint status of ten independent subclones derived from the Hct-116 parental line was analysed and determined to be normal, which excludes clonal variation as the cause of the checkpoint defect in Hct-*MAD2*$^{+/-}$ clones (data not shown).

MAD2 arrests cells in metaphase by associating with the anaphase-promoting complex (APC), thereby inhibiting its ubiquitin ligase activity[12–14]. On release from the checkpoint, progression into anaphase and sister-chromatid separation requires APC^{Cdc20}-dependent degradation of Pds1, or securin[15,16]. Checkpoint-challenged mutant cells containing catalytically active APC are expected to degrade securin prematurely; indeed, after release from a double thymidine block into nocodazole, Hct-*MAD2*$^{+/-}$ cells fail to accumulate the high levels of securin seen in wild-type cells (Fig. 2a). As the mutant cells exit mitosis, the observed loss of Cdc2 activity is not accompanied by a concomitant decrease in cyclin B protein levels (data not shown). As phosphorylation of CDC28 in yeast is a potential mechanism of mitotic exit in checkpoint-challenged cells[17] (see also ref. 18), we performed immunoblots using antisera specific for phosphorylated forms of Tyr 15 on Cdc2 . We observed no increases in Tyr 15 phosphorylation, nor were we able to detect by co-immunoprecipitation any significant decreases in cyclin-B-associated Cdc2 protein levels between 12 and 16 h when the decline in kinase activity is most pronounced (Fig. 2b and data not shown). Further studies are required to determine the precise mechanism of mitotic exit in checkpoint-challenged mammalian cells.

Sister chromatids that have separated prematurely are a hallmark of a defective mitotic checkpoint and have been observed in yeast *mad2* mutants and *Drosophila bub1* mutants[3,16,19]. Therefore, we looked for evidence of precocious anaphase in checkpoint-deficient cells by preparation of metaphase spreads in the presence of colcemid, a spindle inhibitor. Roughly 20% of mitotic figures from the Hct-*MAD2*$^{+/-}$ cells showed prematurely separated sister chromatids, compared with 1% in wild-type cells (Fig. 3a–d).

We performed chromosome counts on metaphase spreads to test the importance of the mitotic checkpoint on chromosome stability. Hct-*MAD2*$^{+/-}$ cells showed an 80% increase in the frequency of

aneuploid metaphases relative to wild-type Hct-116 cells, which have a relatively stable (45,X) karyotype (Fig. 3e). We did not perform karyotype analysis on cells containing 45 chromosomes, which possibly resulted in an underestimation of the total number of mis-segregation events. Using interphase fluorescence *in situ* hybridization (FISH) with chromosome-specific anti-centromeric probes for several chromosomes statistically significant differences in chromosome numbers ($P < 0.008$ to $P < 0.00001$, by Fisher exact test) were identified between wild-type and Hct-*MAD2*$^{+/-}$ cells (Fig. 4a, b). We did not identify differences for chromosome 17 (data not shown). The mechanism of chromosome mis-segregation in checkpoint-defective Hct-*MAD2*$^{+/-}$ cells may be due to premature anaphase even in the absence of spindle inhibitors, but other molecular explanations are possible.

We measured the rates of chromosome loss on clonal populations to determine whether Hct-*MAD2*$^{+/-}$ cells possess a perpetual CIN phenotype, or whether they have acquired an abnormal karyotype as a result of rare events propagated in subsequent generations. We performed chromosome counts on two independently derived wild-type and four Hct-*MAD2*$^{+/-}$ clones after 25 generations. We observed a roughly 100% increase in the rate of chromosome losses in Hct-*MAD2*$^{+/-}$ cells (Fig. 4c). Notably, one of the mutant clones, which has high rates of chromosome instability, has a modal karyotype of 47 chromosomes, possibly reflecting the high degree of karyotypic heterogeneity in the parental Hct-*MAD2*$^{+/-}$ population.

To determine whether the haplo-insufficient effect seen in transformed cells also occurs in primary cells, we studied metaphase spreads from murine embryonic fibroblasts (MEFs) derived from the *Mad2*$^{+/-}$ mouse[5]. MEFs from four out of five *Mad2*$^{+/-}$ mice showed high frequencies of premature sister-chromatid separation

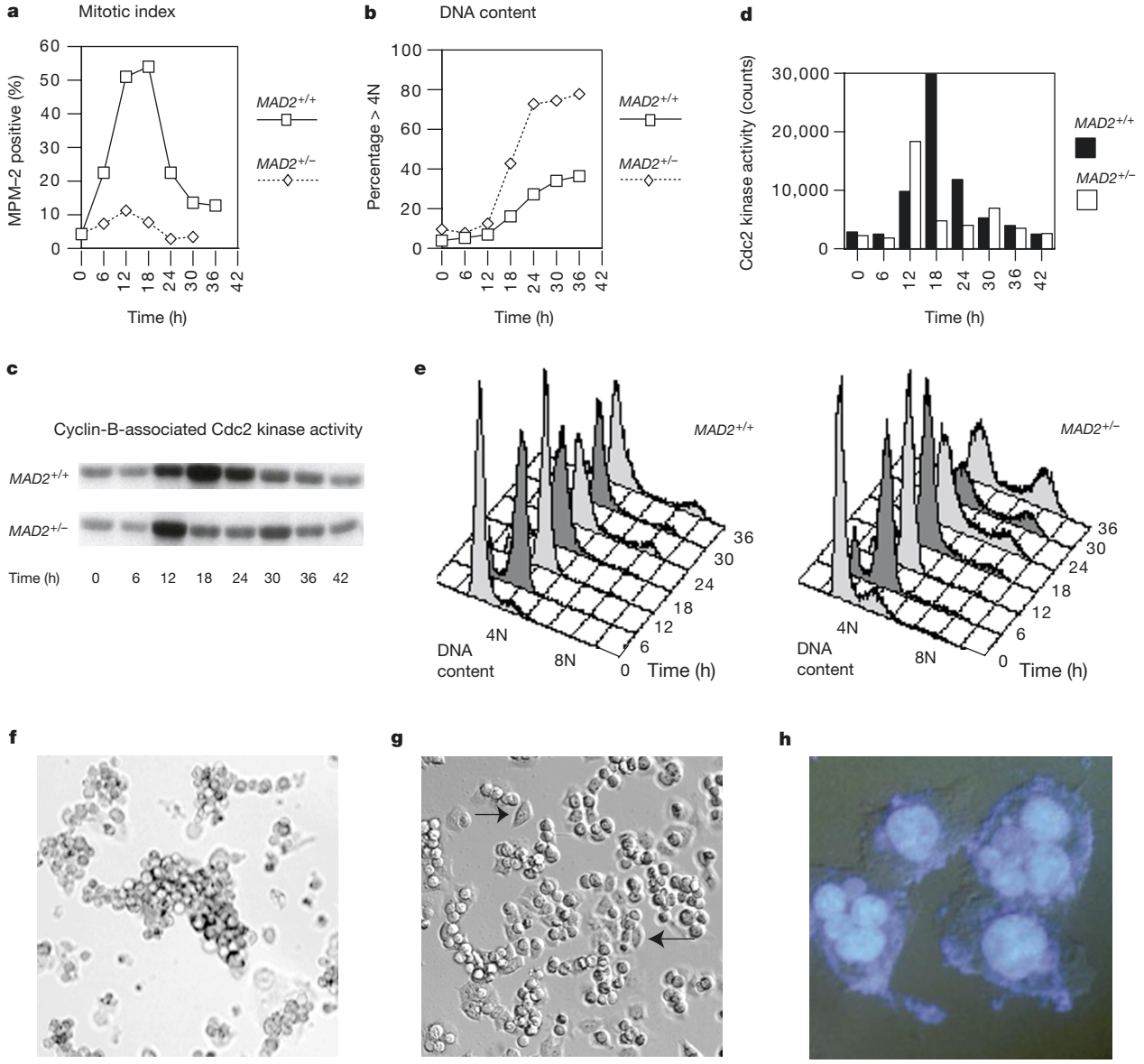

Figure 1 Hct-*MAD2*$^{+/-}$cells have a mitotic checkpoint defect. **a**, **b**, FACS profile of unsynchronized human Hct-116 and Hct-*MAD2*$^{+/-}$cells treated with nocodazole and stained with MPM-2 (**a**) and with propidium iodide (**b**). **c**, Cyclin-B-associated Cdc2 kinase activity on histone H1 substrate of Hct-116 versus Hct-*MAD2*$^{+/-}$cells synchronized in G1/S by double thymidine block and then released into nocodazole. **d**, Cyclin-B-associated Cdc2 kinase activity from the same time course. **e**, FACS profile of propidium-iodide-stained cells from the same time course. The 42-h time point is not shown because of its similarity to the 36-h time point. **f**, DIC microscopy images of unsynchronized Hct-116 cells exposed to nocodazole for 24 h showing an almost complete absence of adherent cells. **g**, DIC microscopy images of Hct-*MAD2*$^{+/-}$cells that remain attached to the tissue-culture dish after treatment for 24 h. Arrows show adherent cells. **h**, Hct-*MAD2*$^{+/-}$ cells exposed to nocodazole for 52 h and analysed by DAPI staining and immunofluorescence microscopy become multinucleated. Magnification of **f**–**h** × 1,000.

relative to wild-type control cultures (Table 1; see also Supplementary Information). We performed chromosome counts on three of the four MEF *Mad2*$^{+/-}$ cultures and in all cases there was a significant increase in the number of aneuploid cells relative to the controls (Table 1). The percentage of aneuploid cells correlates with the severity of premature sister-chromatid separation, suggesting a direct relationship between the severity of loss of checkpoint control and chromosome mis-segregation (Table 1). We note that Mad2$^{+/-}$ mice develop normally, and blastocysts from *Mad2* heterozygote animals display no evidence of an impaired checkpoint as assayed by reactivity to phospho-histone 3 antibody, but premature sister-chromatid separation was not examined in these experiments[5].

Importantly, a high frequency of papillary lung adenocarcinomas, an extremely rare tumour in most wild-type mouse strains, is identifiable in *Mad2*$^{+/-}$ mice killed between 18 and 19 months of age, which suggests a role for defects in the mitotic checkpoint in tumorigenesis (Table 2)[20]. The background rate of lymphomas seen in ageing mice is unchanged in the heterozygote mice. Why the lung is particularly affected by loss of mitotic checkpoint control, the cause of the latency and the rate of chromosome mis-segregation in these tumours are currently being investigated, and the results are likely to clarify the role of mitotic checkpoints in tumour initiation and progression.

The molecular basis of the CIN phenotype has, until recently, remained obscure[21,22]. Our results indicate that partial loss of the mitotic checkpoint may not only be a direct cause of chromosome instability, but may also contribute to tumorigenesis. Defects in the mitotic checkpoint are common in human cancer and have been identified in colon, lung and breast cancer cell lines[1]. Although *MAD2* mutations have not been detected in colon and lung cancer cell lines with mitotic checkpoint defects[23,24], we show here that subtle differences in MAD2 protein levels markedly alter checkpoint function. Therefore, inactivation of one *MAD2* allele, either by

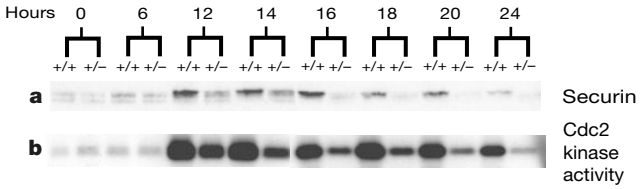

Figure 2 Inappropriate degradation of securin in Hct-*MAD2*$^{+/-}$ cells. **a**, Immunoblot analysis of total cellular protein extract obtained over 24 h from Hct-116 and Hct-*MAD2*$^{+/-}$ cells synchronized by double thymidine block in G1/S and released into nocodazole. **b**, Cyclin-B-associated Cdc2 kinase activity on histone H1 from the same time course. Synchronization and progression through the cell cycle was confirmed by FACS of propidium-iodide-stained cells (data not shown).

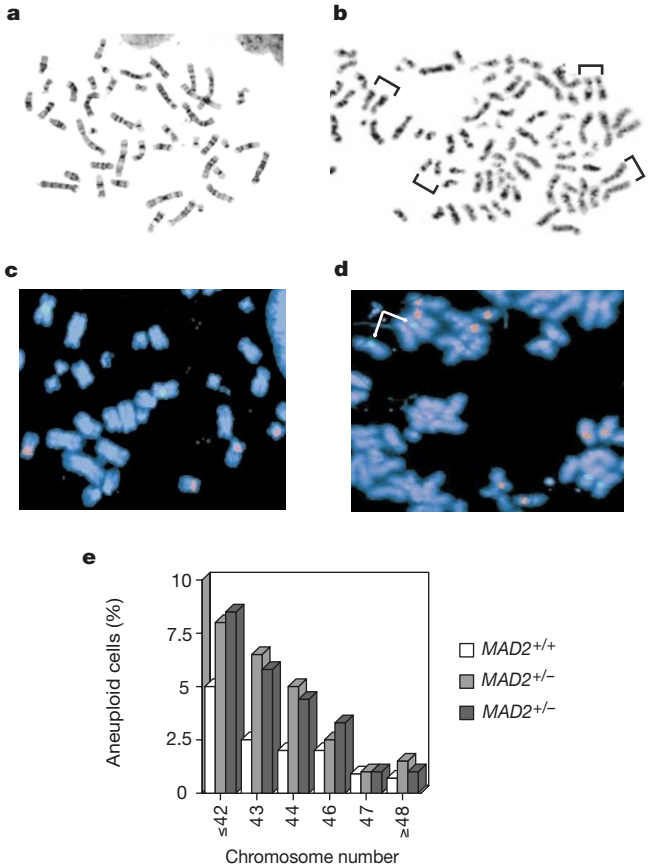

Figure 3 Karyotype analysis of genomic instability in Hct-*MAD2*$^{+/-}$ cell lines. **a**, Normal G-banded metaphase spread from Hct-116 cell lines. **b**, Premature sister-chromatid separation from one Hct-*MAD2*$^{+/-}$ cell line. Brackets show sister chromatids lying separated and adjacent to one another. All of the sister-chromatid pairs are prematurely separated in mitotic figures that show this phenotype. FISH analysis using chromosome-specific FISH probes for CEP 12 (red), CEP 16 (red) and CEP 7 (green), on mitotic figures from the Hct-116 cell line (**c**) and Hct-*MAD2*$^{+/-}$ cell line (**d**). Magnification of **c** and **d**, × 1,000. Arrows indicate a prematurely separated sister-chromatid pair with a third chromatid lying between the two. **e**, Distribution of chromosome numbers of Hct-116 and two Hct-*MAD2*$^{+/-}$ cell lines. At least 400 metaphases were counted for each cell line.

Table 1 Chromosome analysis of mouse embryonic fibroblasts

	Percentage of metaphases with premature sister-chromatid separation $n \geq 100$	Percentage of aneuploid cells
Mad2$^{+/+}$	7	16 (n = 102)
Mad2$^{+/-}$	30	40 (n = 42)
Mad2$^{+/-}$	36	57 (n = 60)
Mad2$^{+/-}$	57	75 (n = 33)

epigenetic silencing or deletion, would be sufficient to create a haplo-insufficient effect and the loss of mitotic checkpoint control. Of note, loss of heterozygosity around 4q27, to which *MAD2* has been mapped, has been identified in several different tumour types[25–28].

Our results also provide a new cytogenetic marker (premature sister-chromatid separation) that should guide screening efforts for the identification of mitotic checkpoint defects in primary tumour samples. Preliminary analysis in primary human cancers has identified such defects (A.C. and V.V.V.S.M., unpublished observations), but further investigation is needed as to whether these are due to subtle decreases in MAD2 levels, or other components of the spindle assembly checkpoint. The precise involvement that a partial loss of mitotic checkpoint function has in the development, progression and management of cancer remains to be determined. As *MAD2*$^{+/-}$ cells become highly aneuploid and continue to cycle after prolonged exposure to spindle inhibitors, checkpoint-defective tumours may be more aggressive and resistant to anti-mitotic chemotherapeutics. Furthermore—and more fundamentally—the long latency period essential for tumour formation in the *Mad2*$^{+/-}$ mice suggests that cooperative mutations at additional oncogenic or tumour-suppressor loci are required to drive transformation in checkpoint-defective cells. Further analysis of the *Mad2*$^{+/-}$ mice should identify these putative genetic interactions. □

Table 2 Tumour frequency in ageing mice

	Lymphomas	Lung tumours
Mad2$^{+/+}$	7.4% (2/27)	0% (0/27)
Mad2$^{+/-}$	9.8% (5/51)	27.5% (14/51)

Wild-type and *Mad2*$^{+/-}$ mice were killed at the age of 18–19 months.

a

Fluorescence *in situ* hybridization analysis
Aneuploid cells (%)

	Chrom. 1	Chrom. 7	Chrom. 8	Chrom. 9	Chrom. 11	Chrom. 12
MAD2$^{+/+}$	3.5	3.1	3.4	1.6	2.8	2.6
MAD2$^{+/-}$	9.7	11.6	6.8	8.9	10.7	12.2
MAD2$^{+/-}$	8.8	10.1	4.2 (NS)	14.8	7.8	12.9

b

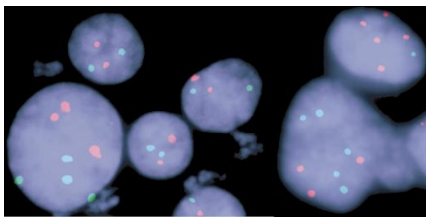

c

Karyotype analysis of cells derived from single-cell clones

	MAD2$^{+/+}$	*MAD2*$^{+/+}$	*MAD2*$^{+/-}$	*MAD2*$^{+/-}$	*MAD2*$^{+/-}$	*MAD2*$^{+/-}$
Modal chromosome no.	45	45	45	45	45	47
Cells deviating from modal number (%)	11	15	32	29	30	50

Figure 4 Interphase FISH analysis using chromosome-specific FISH probes on Hct-116 and Hct-*MAD2*$^{+/-}$ cells. **a**, Summary of six different experiments. 400–600 cells were scored for aneuploidy for each cell line. NS; not significant. **b**, Microscopy image of interphase FISH on Hct-*MAD2*$^{+/-}$ cells using probes for chromosomes 7 (green) and 8 (red) showing three normal and three aneuploid cells. Magnification × 1,000. **c**, Chromosome counts from metaphase spreads on cell populations derived from single cell Hct-116 and Hct-*MAD2*$^{+/-}$ clones after 25 generations. Roughly 100 metaphases were counted for each cell line.

Methods

Cell-cycle analysis and Cdc2 kinase assays

We placed asynchronous cells in 200 ng ml^{-1} nocodazole, and then fixed in 70% ethanol at the given time points. Cells were stained with anti-MPM-2 mouse monoclonal antibody (Upstate Biotechnology), washed and stained with goat anti-mouse fluorescein isothiocyanate (Sigma) and propidium iodide. We performed cell synchronization and H1 kinase assays as described[14]. Detached cell populations were collected and combined with adherent cells for all experiments.

Protein and immunoblot analysis

We prepared total cellular protein extracts as described[14]. For securin, cyclin B and anti-Tyr 15 Cdc2 immunoblots, 30 μg of total cellular extract was resolved by SDS–polyacrylamide gel electrophoresis, transferred to nitrocellulose, and probed with rabbit anti-securin polyconal antibodies, rabbit anti-cyclin B polyclonal antisera, (Santa Cruz), or phospho-specific anti-Cdc2 (Tyr 15) rabbit polyclonal antibodies (New England Biolabs). Horseradish-peroxidase were conjugated donkey anti-rabbit antisera (Amersham) used as secondary antibody, and immunodetection was accomplished by enhanced chemiluminescence (Amersham).

Methods for karyotype, FISH and microscopy

We performed metaphase spreads and Giemsa staining as described[29]. We carried out FISH using chromosome-specific centromeric probes obtained from Vysis, in accordance with the manufacturer's protocol. We analysed slides stained with DAPI counterstain with a Nikon Eclipse 600 microscope attached to an applied imaging cytovision imaging system. We obtained mouse embryonic fibroblasts from 13.5-day-old embryos and used them at passage 3 for metaphase spread preparation as above. For DIC and immunofluorescence microscopy, live cells or cells fixed with 2% paraformaldehyde and stained with 1 μg ml^{-1} DAPI were visualized with an Axiovert 100M microscope (Zeiss) using DIC imaging.

Animal breeding and tumour analysis

Mad2$^{+/-}$ mice were screened and identified as described[5]. Tissues were collected, fixed in formalin and embedded in paraffin blocks before staining with haematoxylin and eosin, and microscopic analysis.

Received 4 July; accepted 23 October 2000.

1. Li, Y. & Benezra, R. Identification of a human mitotic checkpoint gene: hsMAD2. *Science* **274,** 246–248 (1996).
2. Rieder, C. L., Cole, R. W., Khodjakov, A. & Sluder, G. The checkpoint delaying anaphase in response to chromosome monoorientation is mediated by an inhibitory signal produced by unattached kinetochores. *J. Cell Biol.* **130,** 941–948 (1995).
3. Basu, J. *et al.* Mutations in the essential spindle checkpoint gene bub1 cause chromosome missegregation and fail to block apoptosis in *Drosophila*. *J. Cell Biol.* **146,** 13–28 (1999).
4. Kitagawa, R. & Rose, A. M. Components of the spindle-assembly checkpoint are essential in *Caenorhabditis elegans*. *Nature Cell Biol.* **1,** 514–521 (1999).
5. Dobles, M., Liberal, V., Scott, M., Benezra, R. & Sorger, P. Chromosome missegregation and apoptosis in mice lacking the mitotic checkpoint protein Mad2. *Cell* **101,** 635–645 (2000).
6. Kalitsis, P., Earle, E., Fowler, K. J. & Choo, K. H. Bub3 gene disruption in mice reveals essential mitotic spindle checkpoint function during early embryogenesis. *Genes Dev.* **14,** 2277–2282 (2000).
7. Lengauer, C., Kinzler, K. W. & Vogelstein, B. Genetic instabilities in human cancers. *Nature* **396,** 643–649 (1998).
8. DeVita, V., Hellman, S. & Rosenberg, S. (eds) *Cancer—Principles and Practice* (Lipincott-Raven, New York, 1997).
9. Cahill, D. P. *et al.* Mutations of mitotic checkpoint genes in human cancers. *Nature* **392,** 300–303 (1998).
10. Lengauer, C., Kinzler, K. W. & Vogelstein, B. Genetic instability in colorectal cancers. *Nature* **386,** 623–627 (1997).
11. Waldman, T., Lengauer, C., Kinzler, K. W. & Vogelstein, B. Uncoupling of S phase and mitosis induced by anticancer agents in cells lacking p21. *Nature* **381,** 713–716 (1996).
12. Li, Y., Gorbea, C., Mahaffey, D., Rechsteiner, M. & Benezra, R. MAD2 associates with the cyclosome/anaphase-promoting complex and inhibits its activity. *Proc. Natl Acad. Sci. USA* **94,** 12431–12436 (1997).
13. Fang, G., Yu, H. & Kirschner, M. W. The checkpoint protein MAD2 and the mitotic regulator CDC20 form a ternary complex with the anaphase-promoting complex to control anaphase initiation. *Genes Dev.* **12,** 1871–1883 (1998).
14. Wassmann, K. & Benezra, R. Mad2 transiently associates with an APC/p55Cdc complex during mitosis. *Proc. Natl Acad. Sci. USA* **95,** 11193–11198 (1998).
15. Zou, H., McGarry, T. J., Bernal, T. & Kirschner, M. W. Identification of a vertebrate sister-chromatid separation inhibitor involved in transformation and tumorigenesis. *Science* **285,** 418–422 (1999).
16. Alexandru, G., Zachariae, W., Schleiffer, A. & Nasmyth, K. Sister chromatid separation and chromosome re-duplication are regulated by different mechanisms in response to spindle damage. *EMBO J.* **18,** 2707–2721 (1999).
17. Rudner, A. D. & Murray, A. W. The spindle assembly checkpoint. *Curr. Opin. Cell Biol.* **8,** 773–780 (1996).

18. Rudner, A. D., Hardwick, K. G. & Murray, A. W. Cdc28 activates exit from mitosis in budding yeast. *J. Cell Biol.* **149,** 1361–1376 (2000).
19. Minshull, J. *et al.* Protein phosphatase 2A regulates MPF activity and sister chromatid cohesion in budding yeast. *Curr. Biol.* **6,** 1609–1620 (1996).
20. Tuveson, D. A. & Jacks, T. Modeling human lung cancer in mice: similarities and shortcomings. *Oncogene* **18,** 5318–5324 (1999).
21. Zhou, H. *et al.* Tumour amplified kinase STK15/BTAK induces centrosome amplification, aneuploidy and transformation. *Nature Genet.* **20,** 189–193 (1998).
22. Spruck, C. H., Won, K. A. & Reed, S. I. Deregulated cyclin E induces chromosome instability. *Nature* **401,** 297–300 (1999).
23. Takahashi, T. *et al.* Identification of frequent impairment of the mitotic checkpoint and molecular analysis of the mitotic checkpoint genes, hsMAD2 and p55CDC, in human lung cancers. *Oncogene* **18,** 4295–4300 (1999).
24. Cahill, D. P. *et al.* Characterization of MAD2B and other mitotic spindle checkpoint genes. *Genomics* **58,** 181–187 (1999).
25. Krishnan, R. *et al.* Map location and gene structure of the *Homo sapiens* mitotic arrest deficient 2 (MAD2L1) gene at 4q27. *Genomics* **49,** 475–478 (1998).
26. Rashid, A. *et al.* Genetic alterations in hepatocellular carcinomas: association between loss of chromosome 4q and p53 gene mutations. *Br. J. Cancer* **80,** 59–66 (1999).
27. Dohner, H., Bloomfield, C. D., Frizzera, G., Frestedt, J. & Arthur, D. C. Recurring chromosome abnormalities in Hodgkin's disease. *Genes Chromosom. Cancer* **5,** 392–398 (1992).
28. Shivapurkar, N. *et al.* Multiple regions of chromosome 4 demonstrating allelic losses in breast carcinomas. *Cancer Res.* **59,** 3576–3580 (1999).
29. Verma, R. & Babu, A. *Human Chromosomes: Principles and Techniques* (McGraw Hill, New York, 1995).

Supplementary information is available on *Nature*'s World-Wide Web site (http://www.nature.com) or as paper copy from the London editorial office of *Nature*.

Acknowledgements

We thank M. Kirschner for the anti-securin antibody. A.C. performed all cytogenetic and FISH experiments. This work was supported by an NRSA-NIH grant (L.M.); PRAXISXXI, Portugal (V.L.); International Union Against Cancer (ACS-IFB) Fellowship (A.C.); and grants from the NIH (R.B., B.P., P.K.S. and V.V.V.S.M.). We also thank A. Hata and G. Farmer for technical advice, and H. Thaler for statistical analysis.

Correspondence and requests for materials should be addressed to R.B. (e-mail: r-benezra@ski.mskcc.org).

Pre-meiotic S phase is linked to reductional chromosome segregation and recombination

Yoshinori Watanabe*†‡, Shihori Yokobayashi*, Masayuki Yamamoto* & Paul Nurse‡

* *Department of Biophysics and Biochemistry, Graduate School of Science, University of Tokyo, Hongo, Tokyo 113-0033, Japan*
† *PRESTO, Japan Science and Technology Corporation, Kawaguchi, Saitama 332-0012, Japan*
‡ *Imperial Cancer Research Fund, 44 Lincoln's Inn Field, London WC2A 3PX, UK*

Meiosis is initiated from G1 of the cell cycle and is characterized by a pre-meiotic S phase followed by two successive nuclear divisions. The first of these, meiosis I, differs from mitosis in having a reductional pattern of chromosome segregation[1,2]. Here we show that meiosis can be initiated from G2 in fission yeast cells by ectopically activating the meiosis-inducing network. The subsequent meiosis I occurs without a pre-meiotic S phase and with decreased recombination, and exhibits a mitotic pattern of equational chromosome segregation. The subsequent meiosis II results in random chromosome segregation. This behaviour is similar to that observed in cells lacking the meiotic cohesin Rec8 (refs 3, 4), which becomes associated with chromosomes at G1/S phase, including the inner centromere, a region that is probably critical for sister-centromere orientation[5]. If the expression of Rec8 is delayed to S phase/G2, then the centromeres behave equationally. We propose that the presence of Rec8 in chromatin is required at the pre-meiotic S phase to construct centromeres that behave reductionally and chromosome arms capable of a high level of recombination, and that this explains why meiosis is initiated from G1 of the cell cycle.

The meiosis-inducing regulatory network is well characterized in fission yeast[6–9]. We have found that this network is activated only at G1, which explains why meiosis is initiated only during this phase of the cell cycle (see Supplementary Information). On the basis of these findings, we have developed a method of inducing synchronous meiosis from G2 (G2-exit meiosis) by ectopically activating the meiosis-inducing regulatory network during G2 (see Methods), and have compared G2-exit meiosis with meiosis induced from G1 (G1-exit meiosis) (Fig. 1). The cells entering meiosis from G1 underwent a pre-meiotic S phase, meiotic nuclear divisions and sporulation as expected. By contrast, the cells entering meiosis from G2, after mitotic S phase, failed to undergo DNA replication, but did undergo meiotic nuclear divisions and sporulation (Fig. 1a, b, d).

To characterize G2-exit meiosis, we first monitored spindle pole bodies and showed that they remained unseparated until 4 h, indicating that, as in G1-exit meiosis, the spindle was not formed until just before meiosis I (Fig. 1b, and data not shown). Second, we induced meiosis from G2 in *mei4Δ* mutant. The *mei4* gene is required specifically for meiosis I but is not required for mitosis[10]. The *mei4Δ* cells undergoing G2-exit meiosis all arrested with a single nucleus, establishing that the nuclear divisions were meiotic in character rather than mitotic (data not shown). Third, we examined transcripts of the meiosis-specific genes *rec12*, *rec6*, *rec8*, *spo5*, *mei4* and *spo6*, and found that all were induced during both G1-exit and G2-exit meioses (Fig. 1c). Two genes required for DNA replication, *cdc18* and *cdc22*, were induced only during G1-exit meiosis (Fig. 1c), which was consistent with the fact that G2-exit meiotic cells do not undergo a pre-meiotic S phase. Thus, the normal meiotic transcriptional programme is activated during G2-exit meiosis. Last, we assessed intragenic recombination levels by using two closely linked *ade6* mutations[11]. Recombination levels during G1-exit meiosis were similar to those observed during a normal physiological meiosis, but were 20-fold higher than those observed during G2-exit meiosis. The latter level was similar to, although somewhat higher than, the recombination level observed during a mitotic cell cycle. Measurement of intergenic recombination between *lys1* and *leu2* yielded similar results (see Supplementary Information). We conclude that G2-exit meiosis shows several characteristics of a normal meiosis, although recombination levels are lower.

We next investigated chromosome segregation. The $cdc2^{ts}$ mutation blocks meiosis II, leading to the generation of dyads containing two spores[12], but the $cdc2^{ts}$ allele does not impair meiotic recombination or reductional division at meiosis I (ref. 4, and data not shown). The cessation of meiosis before the second division allows us to distinguish between reductional and equational chromosome segregation during meiosis I (ref. 4). Spores from dyads showed over 80% viability in both G1-exit and G2-exit meioses, but spores from tetrads were only 14% viable in G2-exit meiosis in comparison with 86% viable in G1-exit meiosis (Fig. 1e). Staining of nuclei in G2-exit meiosis with 4,6-diamidino-2-phenylindole (DAPI) indicated that chromosome segregation was equal during meiosis I but unequal during meiosis II (Fig. 1d). To assess whether meiosis I was reductional or equational, the segregation of two centromere-linked markers, *lys1* and *ade6*, was monitored in dyads. In G1-exit meiosis, segregation was predominantly +/+, –/–, which was indicative of reductional segregation (Fig. 1f). The occurrence of some +/–, +/– dyads can be explained by recombination between the markers and the centromeres; recombination in the dyads would be expected to be 8% with *lys1* maker (4 cM from the centromere of chromosome I) and 32% with *ade6* maker (16 cM from the centromere of chromosome III). In contrast, segregation during G2-exit meiosis was entirely equational, as indicated by the presence of exclusively

Supplemental Information

Targeting Vector Construction and Southern Analysis

A genomic clone containing all five coding exons of hs*Mad2* was obtained from a placental genomic library (Stratagene), mapped, and critical regions were sequenced. A 7 kb fragment of the genomic clone beginning 17 bp downstream from the 5' end of the open reading frame and including exon 5 was subcloned into Bluescript (Stratagene), The neomycin gene cassette, excluding an exogenous promoter and an ATG translation start site, was cloned in frame with an XhoI I site in exon 2. The vector was then linearized with NotI and transfected into the Hct-116 parent cell line by lipid mediated transfection (GibcoBrl). 80 colonies were isolated, and 4 of these were found to have undergone a homologous integration event as judged by Southern analysis. For Southern blotting, 10 µg. of genomic DNA was digested with SphI, resolved on a 1% agarose gel, and transferred to a nylon membrane for hybridization with a probe derived from an EcoRI and XmaI fragment lying 5' to the targeting construct.

Figure 1SI. **a**. Southern analysis of the human *MAD2* genomic locus after digestion of DNA with SphI. **b**. Diagram of the promoterless targeting construct and targeting strategy.

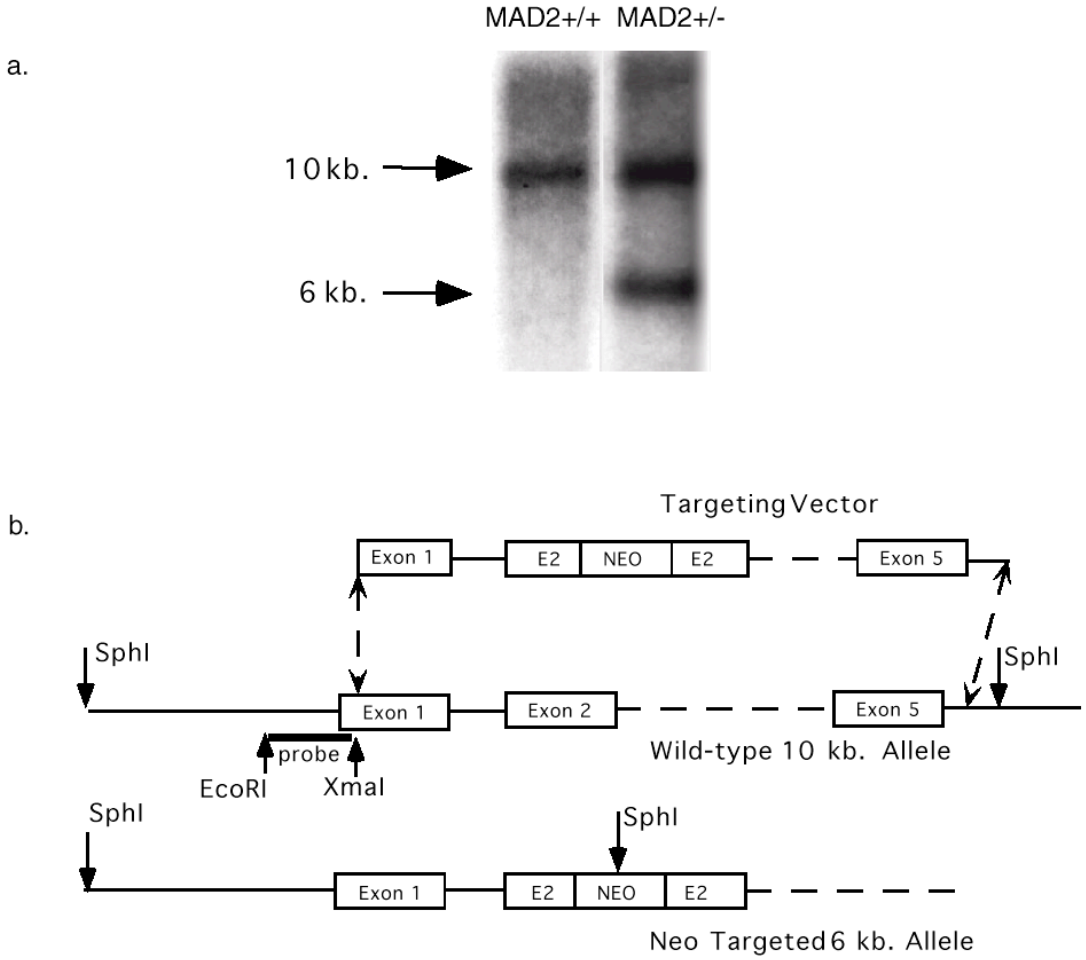

Quantitative Immunoblotting

Total protein lysates were obtained from Hct-116 and Hct-*MAD2+/- cells*, 20-80 ug of protein were resolved by SDS-PAGE, and transferred to nitrocellulose. Membranes were probed with polyclonal anti-rabbit Cdk2 anti-sera (Santa Cruz) and I^{125} conjugated protein A (NEN) was used for quantitative immunodetection. Membranes were incubated in stripping buffer (62.5 mM Tris-Cl, 100 mM ß-ME, 2%

sodium dodecyl sulfate), and reprobed with polyclonal rabbit anti-Mad2 anti-sera. Phosphoimager counts were detected using a Storm 820 Phosphoimager (Molecular Dynamics). Counts were normalized to Hct-116 MAD2 protein levels by the formula MAD2 counts/Cdk2 counts=1 using the ImageQuant Program (Molecular Dynamics).

Figure 2SI. Phosphoimager image of a representative immunoblot performed as described with the associated phosphoimager counts.

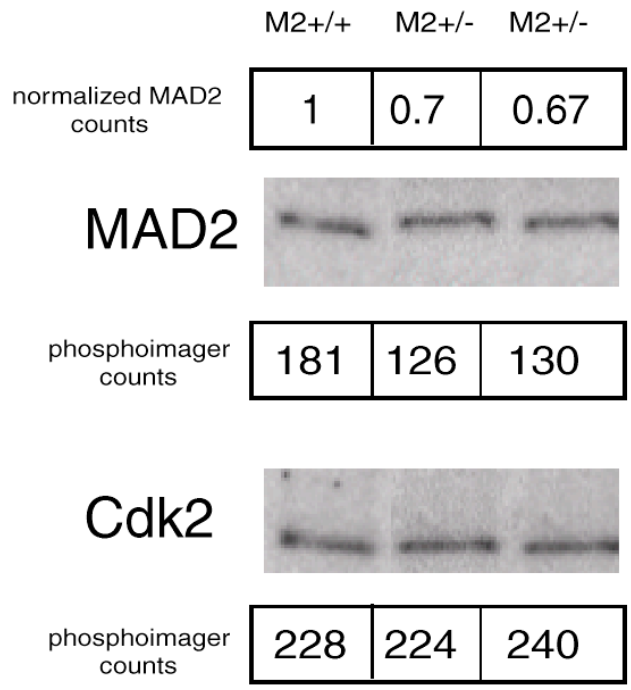

Figure 3SI. Mitotic figures from MEFs with normal sister chromatid cohesion (**a**), and a representative spread from *Mad2* +/- mice displaying prematurely separated sister chromatids (**b**).